Chapter 20
Confocal Raman Imaging of Polymeric Materials

Ute Schmidt, Jörg Müller and Joachim Koenen

Abstract Polymers play an essential role in modern materials science. Due to the wide variety of mechanical and chemical properties of polymers, they are used in almost every field of application and are still a dynamic area in the development of new materials with demanding requirements. Raman spectroscopy is one of the standard characterization techniques used to uniquely determine the chemical composition of a polymer. Modern materials, however, are generally heterogeneous, in which various chemical components or polymorphs of the same chemical species can be present in a very small sample volume. For the analysis of such heterogeneous materials, the combination of Raman spectroscopy with confocal microscopy delivers information about the spatial distribution of the various chemical species with a resolution down to 200 nm. The aim of this contribution is to demonstrate the power of confocal Raman imaging for the characterization of heterogeneous polymeric materials. The first section will deal with polymorphs of polypropylene in polymer films, followed by the nondestructive analysis of polymer blends. A later section will deal with multi-layer polymer coatings and paints and finally, various additives to polymer matrices will be discussed.

20.1 Introduction

The characterization of heterogeneous systems on the microscopic scale continues to grow in importance and to impact key applications in the fields of materials science, nanotechnology and catalysis. The development of advanced polymeric materials for applications such as these requires detailed information about their physical and chemical properties on the nanometer scale. However, some details about the

U. Schmidt (✉) · J. Müller · J. Koenen
WITec GmbH, Lise-Meitner-Strasse 6, 89081 Ulm, Germany
e-mail: ute.schmidt@witec.de

J. Müller
e-mail: joerg.mueller@witec.de

J. Koenen
e-mail: joachim.koenen@witec.de

J. Toporski et al. (eds.), *Confocal Raman Microscopy*, Springer Series in Surface Sciences 66, https://doi.org/10.1007/978-3-319-75380-5_20

phase separation process in polymers are difficult to study with conventional characterization techniques due to the inability of these methods to chemically differentiate materials with sufficient spatial resolution and without damage, staining or preferential solvent washingwq. One technique that has been used successfully in the characterization of heterogeneity in polymers is Atomic Force Microscopy (AFM) [1–4]. AFM can provide spatial information along and perpendicular to the surface of a polymer film with a resolution on the order of 1 nm. The most commonly used AFM imaging mode for polymers is the intermittent contact mode also known as AC Mode or Tapping Mode [5]. In this AFM imaging mode the cantilever is oscillated at its resonance frequency and the topography of the surface is scanned by keeping the oscillation damping constant. A phase image can be recorded simultaneously with the surface topography. In this image, the phase shift between the free oscillation of the cantilever in air and the oscillation while the tip is in contact with the surface is recorded [6]. Since the phase shift depends as much on the viscoelastic properties of the sample as on the adhesive potential between sample and tip, the phase image outlines domains of varying material contrast without describing the nature of the material properties [7–11]. Nevertheless, phase images are often used to characterize polymers at high-resolution [12, 13]. If a composite material consists of compounds with similar mechanical properties, a clear assignment of the phases to the corresponding materials by AFM is quite challenging. To discriminate between materials with similar mechanical properties, additional spectroscopic information is useful. On the macroscopic scale, Raman spectroscopy has become widely used for the characterization of chemical and structural features of polymeric materials [14]. The tremendous value of the Raman effect lies in the fact that the difference in energy between the elastically scattered photons and the Raman shifted photons is caused by the excitation or annihilation of a specific molecular vibration. This energy shift is characteristic for the type and coordination of the molecules involved in the scattering process. Raman spectra provide qualitative and quantitative information about various polymer features [15–17] such as:

- chemical nature: structural units, type and degree of branching, end groups, additives
- conformational order: physical arrangement of the polymer chain
- state of order: crystalline, mesomorphous and amorphous phases
- orientation: type and degree of polymer chain and side group alignment in anisotropic materials.

However, in most spectroscopy setups the spatial resolution is very poor because the excitation laser spot diameter is on the order of 100 μm. Optical microscopy, on the other hand, is capable of providing spatial resolution down to 200 nm using visible light excitation. In a confocal microscope, the light from the sample is detected through a pinhole at the back focal plane of the microscope, giving rise to depth resolution and a strongly reduced background signal [18]. By combining a high-throughput confocal microscope with an extremely sensitive Raman spectroscopy system, it is possible to obtain Raman spectra from extremely small sample volumes down to 0.004 μm^3 as will be shown later. To collect high-resolution Raman images,

the sample is scanned point by point and line by line through the excitation focus [18]. Thus, the Confocal Raman Microscope (CRM) combines the chemical sensitivity of Raman spectroscopy and the high-resolution of confocal microscopy, providing an ideal tool for the characterization of materials in the sub-micrometer range. To achieve the highest resolution, the CRM can be extended with AFM capabilities which enable the user to link the chemical information obtained by confocal Raman spectroscopy with the ultra-high spatial and topographical information acquired by AFM.

The Raman experiments presented in this chapter were performed with a WITec alpha300RA (combined Raman-AFM) using green excitation (532 nm) and a 100×, NA = 0.9 objective. The AFM measurements were done using the same instrument in AFM-AC mode.

20.2 Raman Imaging of Isotactic Polypropylene (IPP)

Polypropylene (PP) is a thermoplastic polymer synthesized from the monomer propylene with the chemical formulas shown in Fig. 20.1. Its dual functionality as plastic and fiber leads to its varied fields of application. As a plastic it is used as reusable containers, stationary plastic parts, laboratory equipment, automotive components, banknotes, etc. As a fiber, polypropylene is used to make ropes, unwoven textiles, packaging materials, etc. The large number of end use applications for PP are due to the ability to tailor grades with specific molecular properties and additives during its manufacturing processes.

The characterization of the morphology of polypropylene fibers in complex structures remains a focus of ongoing research. The crystallinity and the extent of orientation of molecular chains are two of the most important morphological characteristics

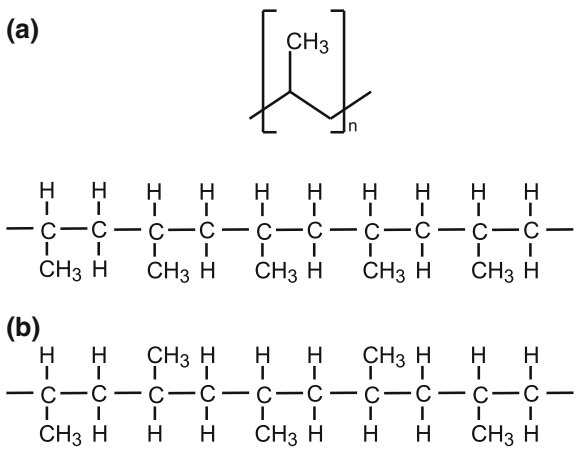

Fig. 20.1 Chemical formula of the polypropylene monomer (**a**) and short segments of polypropylene showing isotactic (upper row) and syndiotactic (lower row) tacticity (**b**)

of the fiber structure that influence the final properties. Raman spectroscopy is one of the many methods used to characterize the microstructure of a semicrystalline polymer. It provides the capability to probe the conformational states of polymer chains in its micro-environment [19–21]. Differences in the Raman spectrum of chains in non-crystalline regions with conformational irregularities or non-helical conformations can be expected [22–25]. A theoretical determination of the vibrational Raman bands of helical polypropylene chains can be found in [26, 27], whereas stress-induced deformations of polypropylene chains are reported in [28, 29]. The structure of a polymer is given by its particular structural arrangement [30]. In isotactic polypropylene, a crystallizable polymer, the structural arrangement is given by the arrangement of crystalline and amorphous domains. The formation of crystalline and amorphous domains is influenced by the crystallization conditions. Crystallization from the unstressed melt results in a randomly nucleated spherulitic structure, whereas crystallization which occurs in an extensional flow field (e.g. during the extrusion process) results in a row-nucleated structure. Depending on the extrusion conditions, bundles of oriented fibers can be formed.

To determine a correlation between the orientation of lammelar rows of isotactic polypropylene and Raman spectra, a uniaxially drawn isotactic polypropylene film (OPP) with a thickness of 50 μm was investigated using polarized Raman spectroscopy. High-resolution atomic force microscopy measurements on such films show a highly oriented fibrillar structure, which is oriented in parallel to the extrusion direction [31]. On this highly oriented isotactic polypropylene film, polarization-dependent Raman spectra were recorded. Figure 20.2 shows a schematic of the four different geometries in which Raman spectra were recorded.

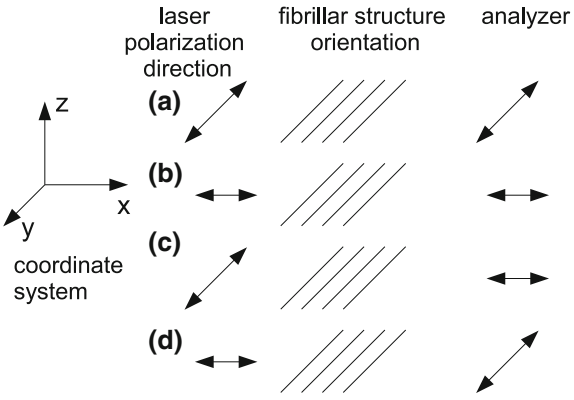

Fig. 20.2 Schematics of the scattering geometry defined in the above shown coordinate system, the incident laser propagates in z-direction. By using a half-wave plate the incident laser light can be polarizes in x- or y-direction. The scattered light is analyzed either in parallel or perpendicular to the polarization direction of the incident laser light. The four possible combinations with respect to the orientation of a one dimensional structure is presented: incident light polarization and analyzer oriented in parallel with the one dimensional structure (**a**), incident light polarization and analyzer oriented perpendicular to the one dimensional structure (**b**), polarization direction of laser and analyzer arranged perpendicular to each other in the two possible arrangements with the one-dimensional structure (**c**, **d**)

The polarized Raman spectra from the OPP film are presented in Figs. 20.3 and 20.4. The spectra result from one sample position. A half-wave plate was used to rotate the polarization of the incident laser light either parallel or perpendicular to the fiber, whereas the scattered light passed through an analyzer either in parallel or perpendicular to the polarization direction of the incident laser light. All recorded Raman spectra were normalized to the bands at 1435 and 1457 rel. cm^{-1}, which are not polarization-dependent. These bands are assigned to methyl group deformations in isotactic polypropylene and show an additional splitting only at very low temperatures [19].

The spectra shown in Fig. 20.3 are recorded in the configuration in which the polarization direction of the incident and scattered laser light are in the same direction, whereas in Fig. 20.4 the spectra recorded in the crossed orientation of laser polarization direction and analyzer are presented. The two later configurations show only minor differences in Raman band intensities as reported before by [20, 32]. Fiber orientation and laser polarization-dependent changes can be clearly observed in the spectra shown in Fig. 20.3. The Raman bands at 809, 841 and 1152, 1169 rel. cm^{-1} are the most characteristic of a directional ordering of the polymer chains in

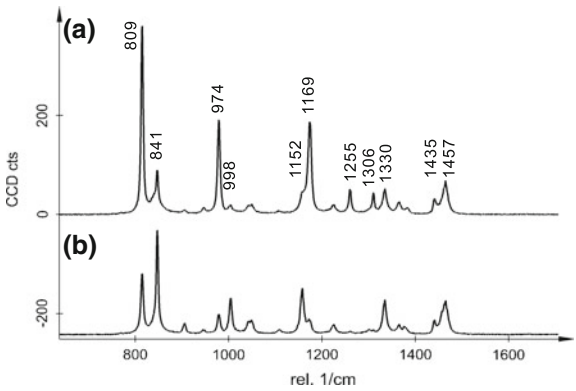

Fig. 20.3 Polarization dependent Raman spectra of uniaxial isotactic polypropylene: polarization direction of laser, fiber and analyzer oriented in parallel (**a**) and polarization direction of laser and analyzer oriented perpendicular to the iPP fibers (**b**)

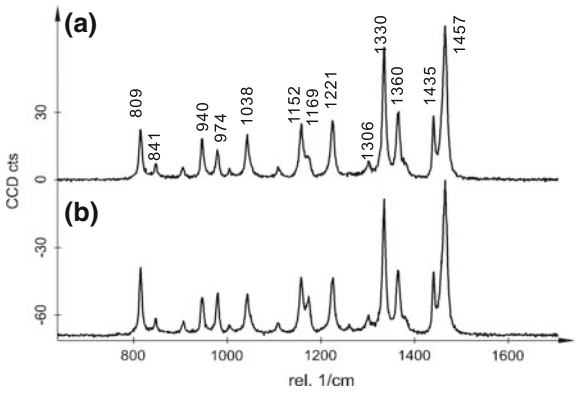

Fig. 20.4 Polarization dependent Raman spectra of uniaxial isotactic polypropylene: polarization direction of laser and fiber oriented in parallel with analyzer perpendicular (**a**) and polarization direction of laser perpendicular and analyzer oriented in parallel to the fiber orientation (**b**)

isotactic polypropylene. Based on normal mode calculations it has been shown that these bands in solid state are associated with the helical chain structure [33, 34].

Considering the above described polarization-dependency of Raman spectra recorded from highly oriented isotactic polypropylene, Raman imaging of polypropylene provides information about the structural arrangement of ordered and disordered polymer chains. Figure 20.5 shows a Raman image of biaxially oriented polypropylene (BOPP). A 2D-array of 100 × 50 single Raman spectra were recorded from a surface area of 50 × 30 μm^2 using a frequency doubled Nd:YAG laser (excitation wavelength 532 nm) and a 100× objective (NA = 0.9). The integration time per single spectrum was 0.1 s. From the 5000 individual spectra, two unique Raman spectra were calculated (Fig. 20.5a). The green spectrum is characteristic for polypropylene fibers oriented parallel to the laser polarization direction, (see Fig. 20.3a), whereas the red spectrum is characteristic for polypropylene fibers oriented perpendicular to the laser polarization direction. The color-coded Raman image (Fig. 20.5b) reveals the oriented fiber bundle. To prove the orientation of such fiber bundles, AFM (Atomic Force Microscopy) measurements were performed on the sample area marked with a frame in Fig. 20.5b. Figure 20.5c shows the topography of the BOPP film, whereas the simultaneously recorded phase image reveals the fiber bundle and the fine fibrillar structure of the BOPP film.

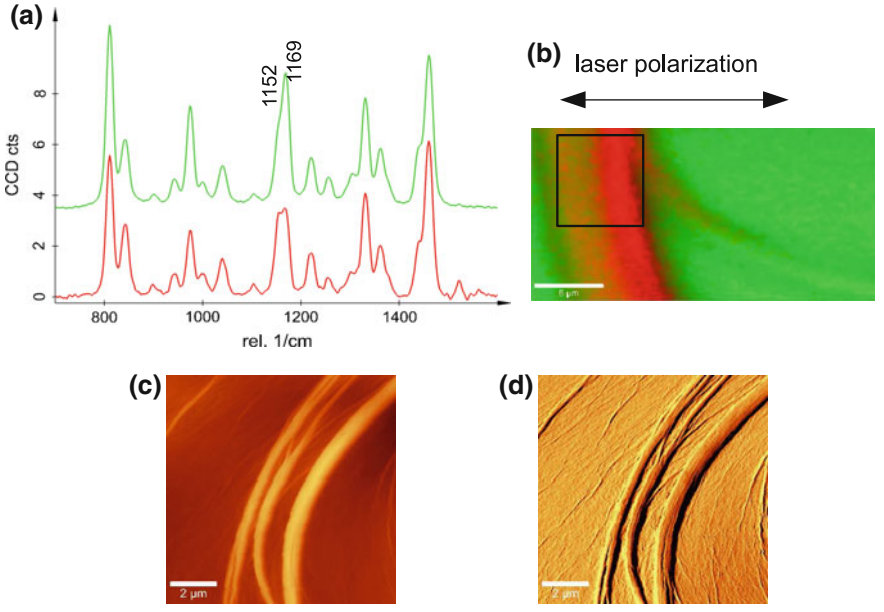

Fig. 20.5 Raman imaging of biaxially oriented polypropylene: Raman spectra (**a**), color-coded Raman image (**b**), AFM topography image (**c**) and AFM phase image (**d**). The scale bar in **b** is 6 µm and in **c** and **d** 2 µm long

The simultaneously recorded phase image reveals much more details of the fine structure of the BOPP film compared to the Raman image. The oriented bundle seems much wider and oriented in a different direction in the Raman image due to the diffraction limited resolution in all three volume directions. The phase image on the other hand is imaging only the surface topography.

Polypropylene films are commonly used as solid dielectrics in high voltage capacitors. Such films are produced by biaxially stretching unstretched molded polypropylene. The surface of such films have an efficiently roughened, fine uneven structure containing crater-like patterns or an isotropic and an anisotropic network structure, which is aligned in the extrusion direction. To obtain more detailed information about the fine structure of such foils, polarized Raman imaging can be employed. By using a polarization rotation (half-wave plate) a surface area can be analyzed using different laser polarization directions, thus determining the different preferential orientation of the spherulitic grains. Figure 20.6 shows the video image recorded on such a foil. The red square marks the area which was scanned for Raman imaging. The spectrometer was equipped with an 1800 grooves/mm grating. Over an area of $15 \times 15\,\mu m^2$, an array of 100×100 Raman spectra was recorded with an integration time of 0.1 s/per spectrum.

The same area was first scanned with the laser polarization and analyzer both oriented horizontally to the x-axis of the image. In a second scan, the same area was scanned with the laser polarization and analyzer oriented both perpendicular to the x-axis of the image. The polarization-dependent Raman spectra of uniaxial isotactic polypropylene (Fig. 20.3) were used as basis spectra for the basis analysis of the recorded 2D spectral arrays [35]. Figure 20.7a shows the distribution of spherulitic structures which are oriented parallel (green) and perpendicular (red) to the laser polarization direction. By rotating the laser polarization direction and analyzer by 90° the image shown in Fig. 20.7b was recorded. In this case, spherulitic structures oriented parallel to the laser polarization direction are shown in yellow, whereas blue was used for perpendicularly oriented spherulitic structures. Figure 20.7c shows

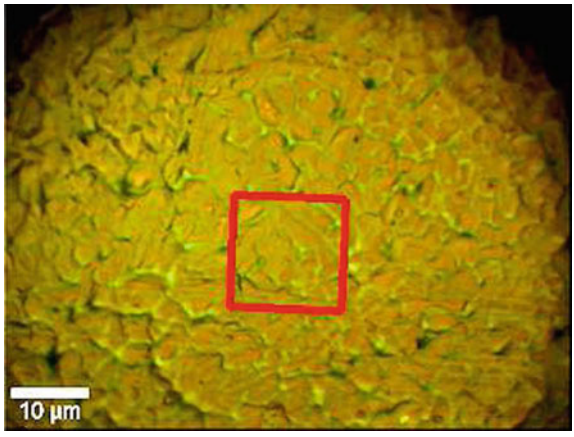

Fig. 20.6 Video image of a polypropylene film used as solid dielectric in capacitors. The red frame marks the area imaged with Raman imaging

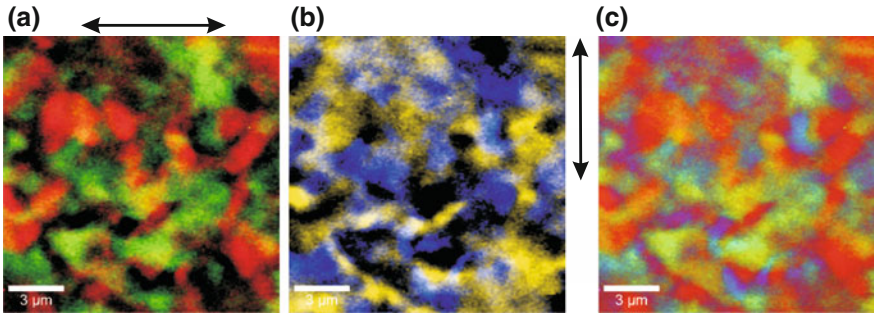

Fig. 20.7 Color coded polarization dependent Raman images of a polypropylene film used as solid dielectric in capacitors: Raman image of polypropylene oriented in parallel and perpendicular to the horizontal (**a**) and vertical (**b**) laser polarization direction and combined color-coded Raman image of all polarization directions

a color-coded image of the various grain orientations detected by using polarized confocal Raman imaging.

The predominant colors in Fig. 20.7c are red and green indicating that one measurement with polarized light is enough to characterize the orientation in such polymer films.

20.3 Raman Imaging of Polymer Blends

Polymer blends are designed to address the needs of different industries and in many cases the relationship between structure, morphology and material properties is crucial for the optimization of material design. Since the beginning of the plastics industry it has been recognized that blending yields materials with property profiles superior to the features of the individual components. A polymer blend is a macroscopically homogeneous mixture of two or more different species of polymer which combine the useful properties of all of the constituents. The technology of blending is now advancing at a rapid pace. There has been progress in the understanding of the behavior of polymer blends, especially the thermodynamics and rheology [36, 37]. New blends are constantly being developed and characterized. The main parameters which influence the properties of a blend are the interface and the morphology. The morphology of a polymer blend indicates the size, shape and spatial distribution of the component phases with respect to each other. The properties, such as: mechanical, optical, rheological, dielectrical, and barrier properties of polymer blends are strongly influenced by the type and granularity of the phase structure. A large variety of analytical methods are used to characterize the morphology of polymer blends. Raman imaging contributes to the analysis of multicomponent polymer systems by visualizing the distribution of individual components based on differences in the unique Raman spectra for different polymeric materials. Domains of different

components in polymer blends are typically of a larger size. In many cases, they are formed during phase separation. Raman imaging provides real-space observation of different coarsening processes and allows direct quantification of phase volume fractions and the computation of domain interface curvatures of various morphologies. A direct assignment of image features to various polymer phases becomes available with a resolution down to 200 nm. Micro-phase separation patterns with spherical, cylindrical, lamellar or micellar morphology, which are characterized by structural factors in the tens of nanometers range can be analyzed by transforming the confocal Raman microscope into an AFM [35, 38].

In the following sections three different blends composed of immiscible polymers, which are at room temperature in either the rubbery or glassy state were investigated. For these studies, thin films of the polymer blends with a thickness of less than 100 nm were prepared by spin-coating solutions containing the polymers onto clean glass cover slides at 2000 rpm.

20.3.1 Raman Imaging of Thin Films of the Polymer Blend: Polystyrene (PS) - Ethyl-Hexyl-Acrylate (EHA)

In this section a polymer blend which consists at room temperature of the glassy state polymer PS and the rubbery state polymer EHA is described.

Figure 20.8a shows the Raman spectra of the pure blend components. Both, PS (blue) and EHA (green) show characteristic band structures around 2800–3000 rel. cm^{-1}, which are associated with C-H stretching and the peak at 1454 rel. cm^{-1} which is characteristic for C-H bending. EHA shows a Raman peak at 1735 rel. cm^{-1} which is characteristic for C=O stretching, whereas PS shows the additional Raman bands associated with the benzene ring modes [39, 40]. These two spectra can be used for the basis analysis of 2-dimensional spectral arrays acquired from the polymer blend.

The variations in the Raman spectra of these two polymers make it possible to distinguish the various polymers from each other when they are blended. The blend of PS-EHA was scanned in Raman spectral imaging mode. Complete Raman spectra were recorded at every image pixel (200×200 spectra) with an integration time of 0.08 s/spectrum. To assign the different polymers in the film, the complete spectra of the two polymers were employed by using basis spectra analysis (see Chap. 5). The distribution of the EHA is shown in Fig. 20.8b, whereas the distribution of PS is represented in Fig. 20.8c. These two complementary Raman images show that PS forms islands surrounded by the EHA matrix. Both polymer phases wet the glass substrate.

High-resolution AFM images recorded on this film are shown in Fig. 20.9. The topography image (Fig. 20.9a) reveals that the PS islands are 40 nm higher than the surrounding EHA phase. The diameter of the PS islands range from 100–1500 nm. The simultaneously recorded phase image (Fig. 20.9b) shows a high phase contrast between the two materials. Brighter areas can be assigned to the harder (glassy)

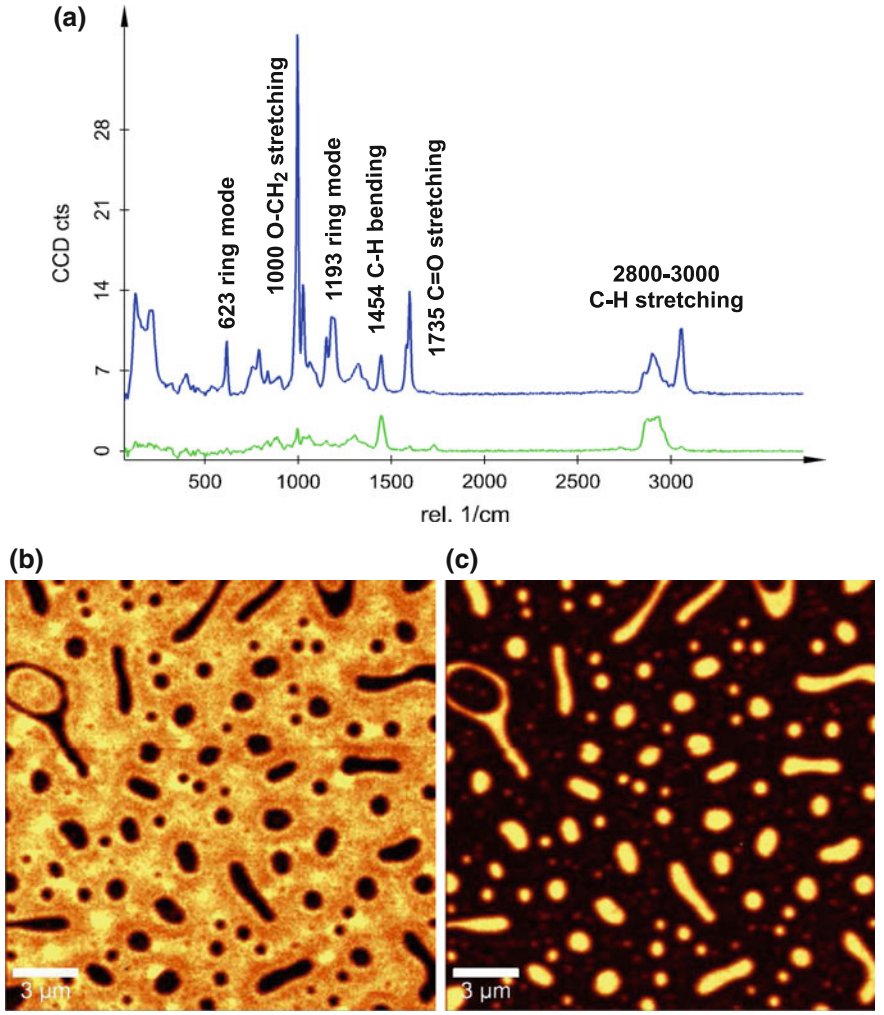

Fig. 20.8 Single Raman spectra of pure PS (blue spectrum) and EHA (green spectrum) (**a**), Raman image of EHA distribution (**b**) and Raman image of PS distribution (**c**)

polystyrene, whereas the soft (rubbery) EHA appears darker. Within the EHA phase a netlike fine structure becomes visible in the phase image.

To determine the overall thickness of the thin film of the polymer blend, the film was scratched with a razor blade and imaged with AFM. Figure 20.10a shows the topography of the scratch and the corresponding height histogram of the image (Fig. 20.10b).

The measured height of the EHA phase of only 30 nm together with the focus spot size of 340 nm shows that a sample volume of less than 0.004 μm^3 is enough to

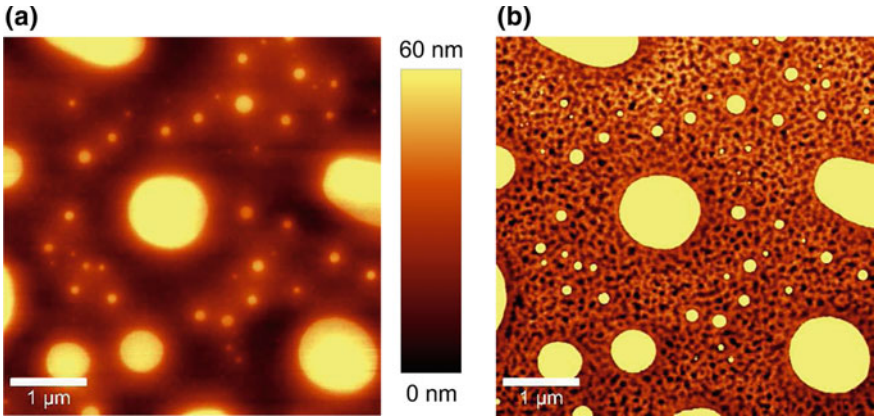

Fig. 20.9 High-resolution AFM AC mode image of the polymer blend PS-EHA: topography image (**a**) and simultaneously recorded phase image (**b**)

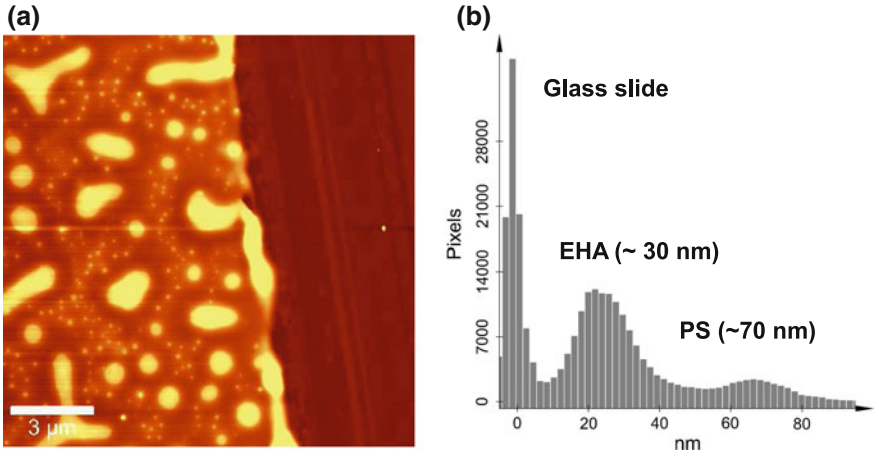

Fig. 20.10 AFM AC mode topography image of the scratched film of PS-EHA (**a**) and histogram of height distribution on the surface (**b**)

identify the chemical species with the confocal Raman microscope using integration times of less than 100 ms/spectrum.

20.3.2 Raman Imaging of Thin Films of the Polymer Blend Ethyl-Hexyl-Acrylate (EHA) - Styrene-Butadiene Rubber (SBR)

In this section a polymer blend consisting of two polymers, which are in the rubber phase at room temperature, is described. A 2D spectral array of 100×50 spectra was acquired from a sample area of $10 \times 5\,\mu m^2$. From the 5000 recorded spectra, two distinct Raman spectra were calculated by using cluster analysis (see Chap. 5 in this book for a more detailed explanation). These spectra are represented in red and green in Fig. 20.11a. The green spectrum shows the characteristic Raman bands of EHA (compare with green spectrum Fig. 20.8a), whereas the red spectrum shows additional Raman bands at 1000 and 3060 rel. cm^{-1} and in the spectral range of 1635–1650 rel. cm^{-1}. The latter Raman bands are associated with C=C stretching and are characteristic for SBR [35]. The differential spectrum between the red and the green spectra is shown in blue in Fig. 20.11a and represents the unique Raman spectrum of SBR [35]. Figure 20.11b shows the Raman image of the distribution of the two detected species within the scanned surface area. The distribution of the pure EHA phase is represented in green and the red color denotes the presence of a mixed phase consisting of EHA and SBR.

To gain insight into the fine structure of the mixed phase consisting of EHA and SBR, high-resolution structural information is required. This can be obtained from high-resolution AFM images. In a previous study it could be shown that phase images recorded on thin films of pure SBR spin-coated on glass substrates reveal a statistical distribution of the hard styrene blocks in the rubbery butadiene matrix [35]. The fine structure of pure EHA wetting the glass substrate is shown in Fig. 20.10b.

AFM images recorded in AC mode on the polymer blend consisting of EHA and SBR reveal a two level topography. The simultaneously recorded phase image is shown in Fig. 20.11c. The netlike structure, characteristic for EHA wetting the glass substrate, could be resolved in the topographic lower regions of the surface. This finding is in good agreement with the elliptic domains consisting of pure EHA found in the Raman image. The topographically elevated structure, consisting of a large network appears featureless if a large area is scanned. The high-resolution AFM image obtained from a smaller scan area (see insert of Fig. 20.11c) reveals a grain-like fine structure in the topographically elevated structure, which is characteristic for SBR. The Raman image showed however, that in these surface areas the two polymers SBR and EHA coexist, thus the SBR phase is formed on top of the EHA layer. By combining confocal Raman imaging with high-resolution AFM imaging, it could be shown that in this polymer blend only EHA is wetting the glass substrate. For this polymer blend only the combination of Raman and AFM imaging reveals the wetting and separation behavior of the two rubbery polymers without selective dissolution of one of the polymer phases.

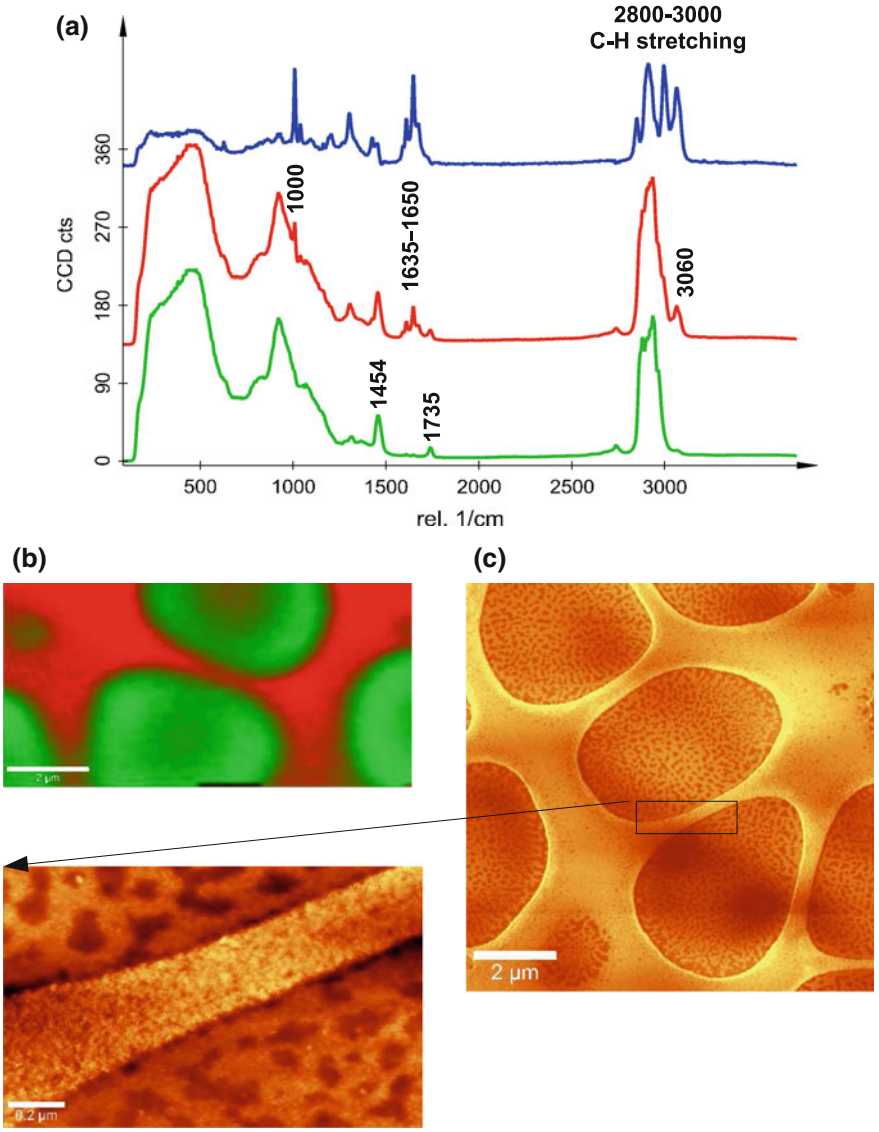

Fig. 20.11 Raman spectra of EHA (green spectrum), a mixed Raman spectrum of EHA+SBR (red spectrum), and the differential spectrum between red and green spectrum revealing the pure SBR Raman spectrum in blue (**a**), color-coded Raman image of the distribution of pure EHA and of the mixed phase EHA+SBR (**b**), and high-resolution AFM phase images of the polymer blend (**c**)

20.3.3 Raman Imaging of Thin Films of the Polymer Blend PS-EHA-SBR

In this section a thin film of a three component polymer blend is described, which at room temperature consists of the two rubbery state polymers EHA and SBR and the glassy state polymer PS.

A 2D spectral array of 128 × 128 spectra was acquired from a sample area of 20 × 20 μm^2 of this polymer film. The spectral array was analyzed using basis analysis. The Raman spectra shown in Fig. 20.12a were used as basis spectra. In the basis analysis technique, each measured Raman spectrum is fitted by a linear combination of a certain number of basis spectra (see also Chap. 5). A color-coded Raman image of the distribution of the three polymer phases is shown in Fig. 20.12b. In this image, blue represents the distribution of PS while the green areas consist of pure EHA. Yellow denotes a mixed phase of EHA and SBR. This image confirms the previously observed phase separation processes: PS, the polymer in the glassy state at room temperature, and EHA, form an interface with the glass substrate, whereas the SBR is formed on top of the EHA phase.

High-resolution AFM images recorded from this blend show that PS is forming a topographically elevated rope-like structure, surrounded by SBR and EHA. A high-resolution AFM phase image (Fig. 20.12c) reveals the fine structures of the three blended polymers. The bright areas of this image can be associated with the hard PS-phase, whereas the dark red reveals the fine structure of EHA, the most adhesive component of the blend. The grain-like fine structure is found again in the SBR layer formed on top of the EHA phase.

A final evaluation of the structural arrangement of the various components of this blend is a confocal Raman depth scan. Figure 20.13 shows a color-coded confocal Raman depth scan performed on this three component polymer blend. For this Raman image a 2D spectral array consisting of 100 × 50 complete Raman spectra was recorded in a plane perpendicular to the surface, similar to a virtual section of the sample. The unique Raman spectra of the blend component (Fig. 20.12a) were used as basis spectra for the basis analysis software tool. Blue and green corresponding to PS and EHA respectively from this image form an interface with the glass substrate, whereas the red SBR phase is formed on top of the green EHA phase.

20.4 Polymer Coatings

Surfaces are coated to give them protection against a hostile environment, to enhance their appearance, or to impart specific properties to the surface. The desired effects can be achieved with coatings ranging from several micrometers to less than one micrometer in thickness. For some surfaces several layers are required to fulfill a specific task, in other cases a specific distribution of materials is needed. Establishing

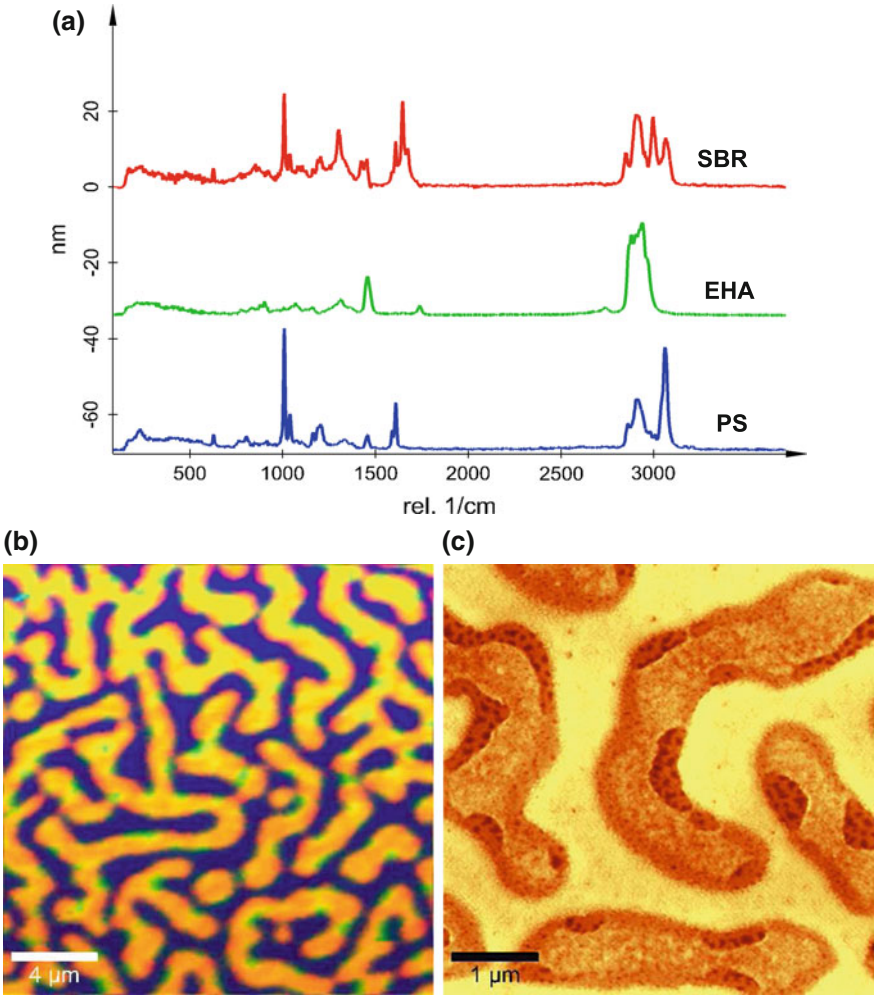

Fig. 20.12 Single Raman spectra of pure PS, EHA, and SBR used as basis spectra for the basis analysis of the 2D spectral array acquired from this sample (**a**), color-coded Raman image of the three component polymer blend (**b**), and high-resolution AFM phase image of this polymer blend (**c**)

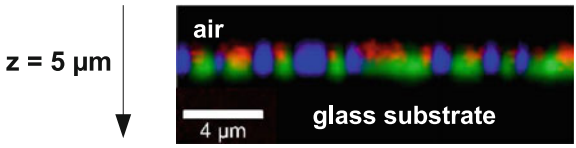

Fig. 20.13 Confocal Raman depth profile of the three component polymer blend consisting of PS (blue), EHA (green), and SBR (red)

the chemical and morphological composition of a surface is therefore a vital step towards understanding its behavior. In the following, several examples of coatings will be presented.

20.4.1 Acrylic Paints

Alkyd and acrylics are used as binders in paints and coatings. These materials produce a shiny, hard finish that is highly water-resistant. Of interest in studying this system are changes in the Raman spectra during the drying process of the paints and the distribution of the two phases within the paint. Figure 20.14 shows Raman spectra recorded from the alkyd phase before drying (a) and in the dry state of the paint (b). The decrease of the Raman bands at 1265 and 3012 rel. cm^{-1} (cis-C=C-H asymmetric stretching bands) and the cis-C=C stretch peak at 1656 rel. cm^{-1} are related to chemical changes during oxidation [41].

Figure 20.15a shows the Raman spectra of alkyd and acrylic latex in their dry state. The small differences in the Raman spectra make it possible to distinguish the two phases in the emulsion. A Raman spectral image consisting of 200 × 200 spectra was recorded from a sample area of 10 × 10 μm^2.

The spectra from Fig. 20.15a were used as basis spectra for the basis spectra analysis of the recorded 2-dimensional spectral array. The resulting color-coded Raman image is presented in Fig. 20.15b. This image indicates that large elliptic domains consisting of alkyd are surrounded by the acrylic latex phase. Figure 20.15c shows the phase image of the dried paint, indicating the stiffer nature of the acrylic latex phase. It also reveals the individual latex spheres, which are smaller than the

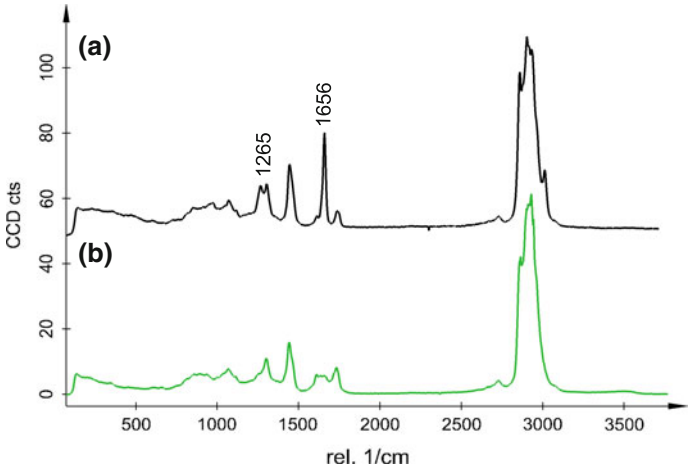

Fig. 20.14 Raman spectra of the alkyd phase before (**a**) and after (**b**) drying of the paint

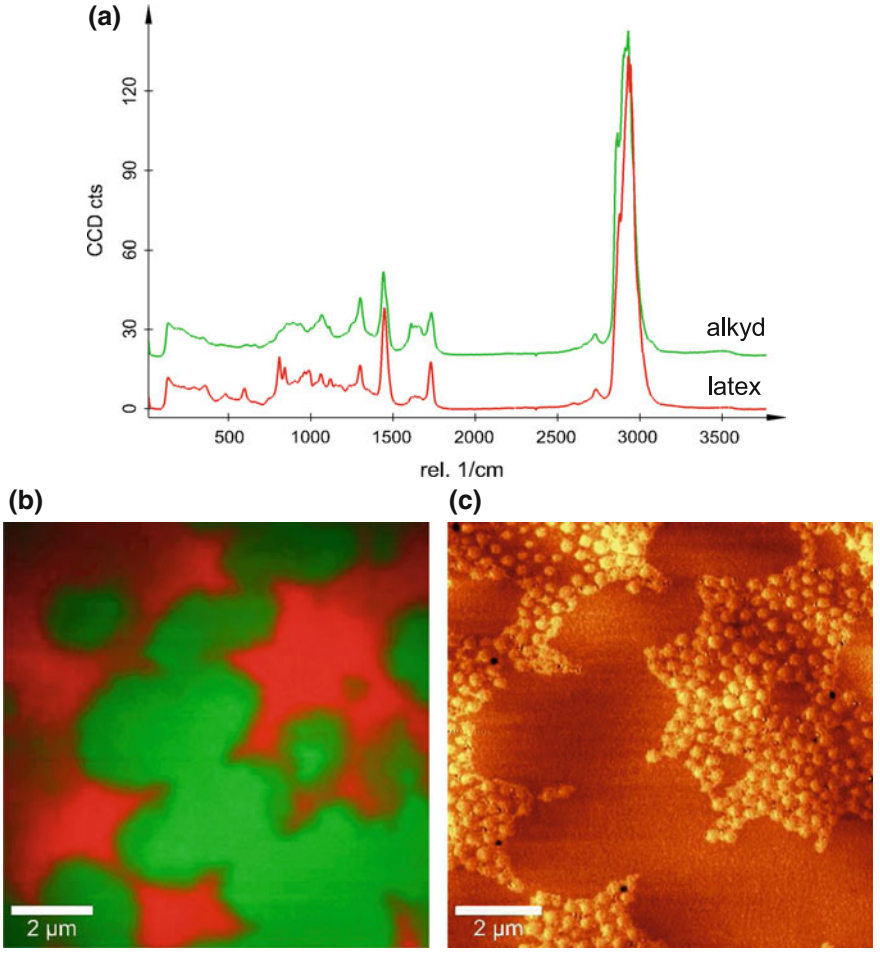

Fig. 20.15 Raman spectra of the alkyd and latex phase in the dry state of the paint (**a**), color-coded Raman spectral image of the paint surface (**b**), and AFM AC mode phase image of the same sample area revealing the spherical latex particles (**c**)

diffraction limit (using an air objective) and are thus not resolved in the confocal Raman image. The diameter of the latex spheres range from 20 to 250 nm.

20.4.2 Adhesives

The use of multi-layered materials for adhesives is now a common practice. Confocal Raman depth scans provide insight into the layered structure of such polymers without any specific sample preparation.

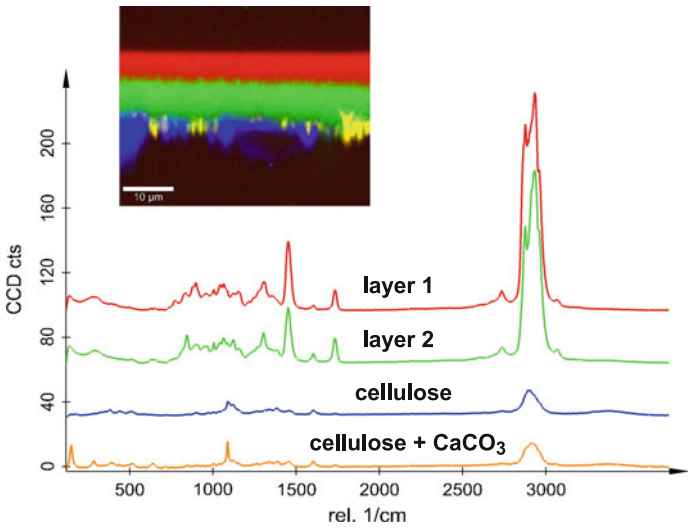

Fig. 20.16 Color coded confocal Raman depth profile of adhesive polymeric layers on a paper substrate

As an example, Fig. 20.16 shows a confocal Raman depth scan performed on an adhesive paper. In this case two polymer layers were applied to the paper surface in order to fulfill the required tasks. The two polymers are immiscible and form a sharp interface (red and green) with the paper beneath (blue and yellow).

20.5 Additives in Polymer Matrices

Nanomaterials are increasingly being used as additives to polymers to simultaneously enhance a variety of properties without sacrificing any qualities of the base polymer.

Additives of inorganic materials in solid form to polymer matrices have a great significance in plastics industry. They are used for a wide variety of purposes, e.g. anti-oxidants, stabilizers, fillers, pigments etc. Anti-oxidants and stabilizers are added in small quantities to prevent degradation of the polymer when it is exposed to air, light and heat. Fillers may be used either simply to produce a cheaper product or to improve the mechanical or electrical properties of the polymeric material. Confocal Raman microscopy allows the allocation of such fillers in the polymer matrix, leading to a better understanding of the properties of the materials. In the following, two examples of fillers are presented.

Fine metal powders and carbon black are commonly added to polymer matrices to improve the electrical, mechanical or thermal properties of the polymers. Figure 20.17 shows a confocal Raman microscopy study of polypropylene with TiO_2 and carbon inclusions. An area of $30 \times 30\,\mu m^2$ of the sample was scanned and a

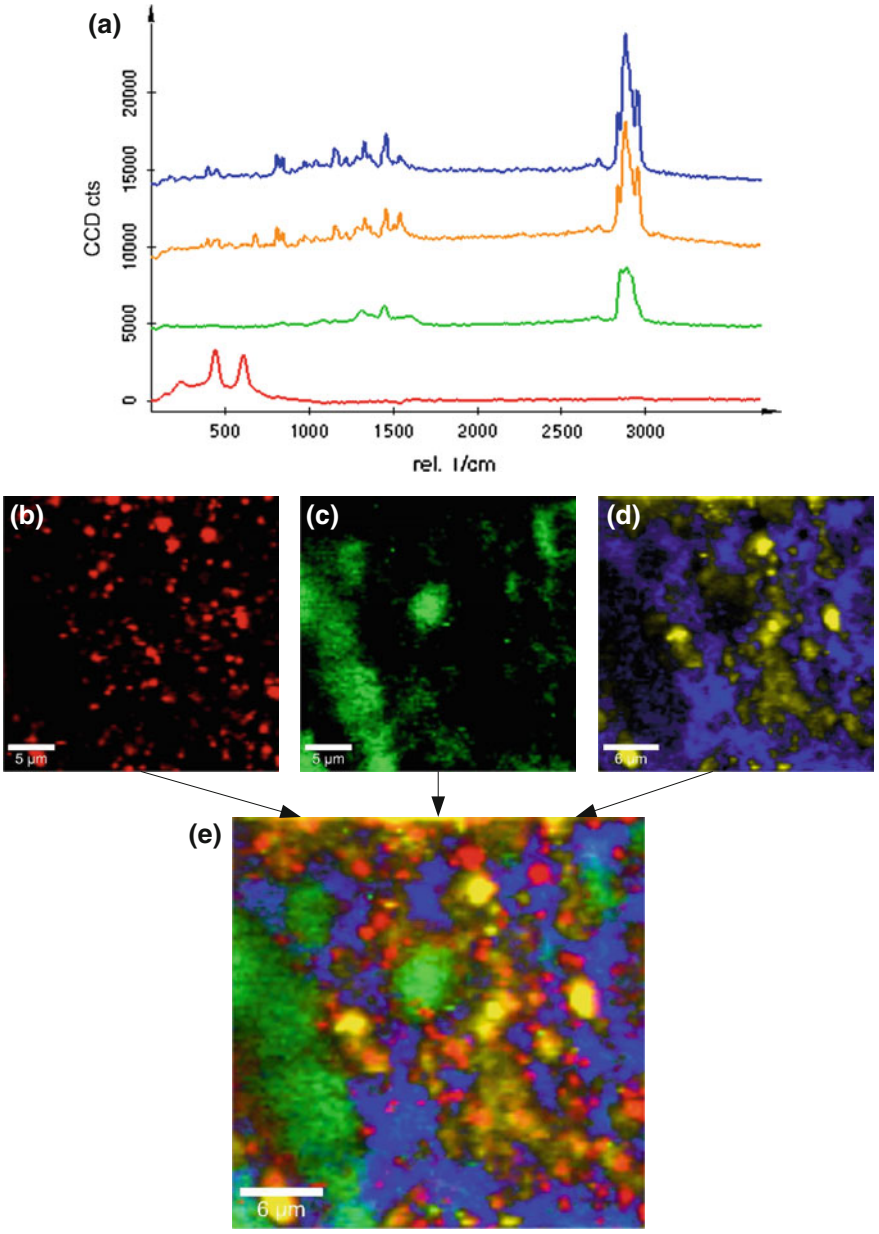

Fig. 20.17 Confocal Raman imaging of additives in a polypropylene matrix: characteristic Raman spectra evaluated from the 2D array of 10,000 spectra using cluster analysis: orientation-dependent PP Raman spectra (blue and yellow), Raman spectrum of amorphous carbon in organic matrix (green) and Raman spectrum of TiO_2 (red) (**a**), distribution of TiO_2 particles (**b**), distribution of amorphous carbon (**c**), distribution of PP (**c**), and color-coded Raman image of the analyzed surface area (**d**)

two-dimensional array of 100 × 100 Raman spectra was acquired with an integration time of 100 ms per spectrum. From this measurement four different spectra were evaluated using cluster analysis. These spectra are presented in Fig. 20.17a. In addition to the orientation-dependent Raman spectra of polypropylene (blue and yellow spectra Fig. 20.17a) the spectrum of TiO_2 (red) and the spectrum of amorphous carbon in an inorganic matrix(green) were extracted by the cluster analysis algorithm.

These spectra were used to evaluate the distribution of each component on the studied sample area using the basis analysis. The weighting factor resulting from the basis analysis denotes the presence of the species in a defined sample volume. Figure 20.17b shows the distribution of TiO_2 on the sample, whereas Fig. 20.17c shows the distribution of amorphous carbon. In Fig. 20.17d the color-coded Raman image of the distribution of polypropylene is presented. By overlaying the images described above and assigning each component the color of the corresponding Raman spectrum, the complete color-coded Raman image can be generated as shown in Fig. 20.17d. From this image it can be clearly seen that the TiO_2 particles adhere to the different oriented polypropylene grains, whereas amorphous carbon forms large clusters with a diameter of up to 6 μm.

Carbon nanotubes (CNTs) have physical properties that exceed those of commonly used materials. With a tensile strength eight times that of stainless steel and a thermal conductivity five times that of copper, CNTs are an obvious choice for creating a new class of composite materials. Their inclusion in a polymer or ceramic matrix holds the potential to enhance the host material's electrical, mechanical, or thermal properties by orders of magnitude, well above the performance possible with traditional fillers such as carbon black or ultra-fine metal powders.

Figure 20.18 shows the distribution of single-walled carbon nanotubes (SWCNTs) in a polymer matrix. For this experiment a diode laser with a wavelength of 785 nm was employed for Raman imaging. An area of 20 × 20 μm^2 was scanned and a two dimensional array of 100 × 100 Raman spectra was acquired with an integration time of 200 ms per spectrum. Figure 20.18a shows the three Raman spectra evaluated with cluster analysis. The Raman spectra of the polymer (red) and two different types of SWCNT's (blue and green) were detected. In this example, only SWCNT's show a Raman band in the spectral range 120–350 rel. cm^{-1}. This Raman band arises from the coherent vibration of the carbon atoms in the radial direction, as if the tube were breathing, and are known as radial breathing modes (RBM). These RBM frequencies (ω_{RBM}) are very useful to identify whether a given carbon material contains SWCNT's and for characterizing the nanotube diameter distribution (d_t) in the sample through use of the relation $\omega_{RBM} = A/d_t + B$, where the A and B parameters are determined experimentally [42, 43]. For typical SWCNT bundles, as expected in this polymer matrix, A = 234 nmcm^{-1} and B = 10 cm^{-1} may be used. The two different ω_{RBM} found in this sample are at 258 and 267 rel. cm^{-1}, corresponding to tube diameters of 0.96 and 0.91 nm respectively. The distribution of these two types of SWCNTs is shown in Fig. 20.18b. The SWCNTs with a diameter of 0.94 nm (green) appear as 2 − 4 μm long rods, whereas the SWCNTs with a diameter of 0.91 nm appear much shorter (0.5 − 1 μm).

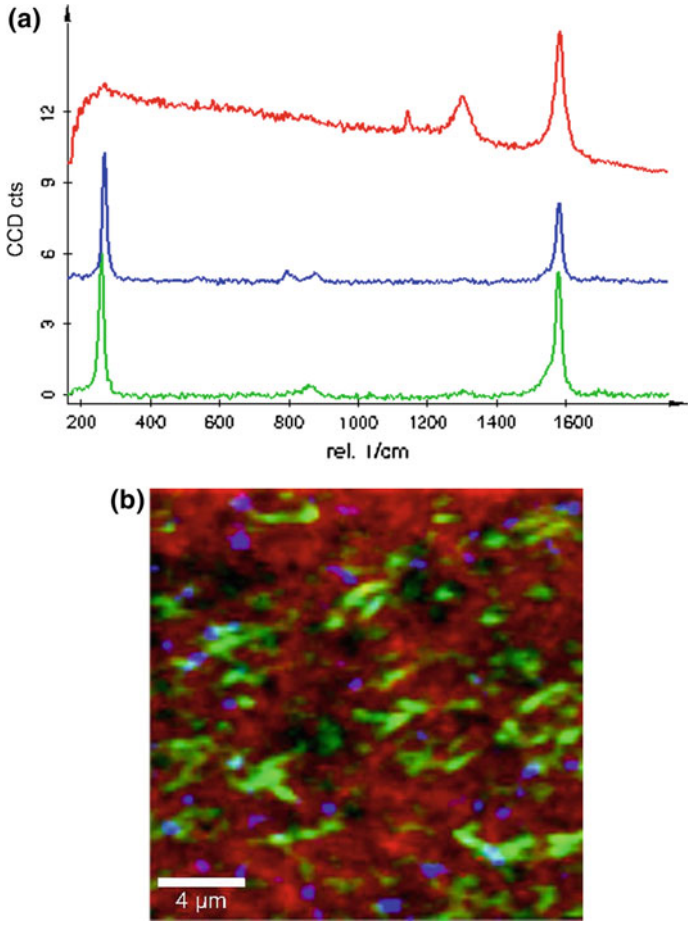

Fig. 20.18 Confocal Raman imaging of the distribution of carbon nanotubes in a polymer matrix: characteristic Raman spectra evaluated from the 2D array of 10000 spectra using the cluster analysis tool of the WITec project software, polymer matrix (red), carbon nanotubes with different diameter (blue, green) (**a**) and color-coded Raman image of the analyzed surface area (**b**)

20.6 Summary

Confocal Raman microscopy is a powerful tool for the characterization of polymeric materials. It could be shown that Raman spectroscopy allows the identification of chemically distinct materials. In combination with a confocal microscope, the distribution of various polymer phases within a polymer matrix can be determined. As shown in Sect. 20.2, confocal Raman microscopy is sensitive to the orientation of long chain polymeric materials, enabling the determination of orientation of fibers when the polarization direction of the excitation laser is known. Polymorphs of a

polymer can be detected and their distribution on the sample visualized. In Sect. 20.3 the combination of confocal Raman microscopy and atomic force microscopy has been demonstrated in the studies of thin films of polymer blends. All studied blends showed a clear phase separation and although the analyzed films were very thin (<100 nm), the sensitivity of the confocal Raman microscope was still high enough to identify the chemical composition of the films with short integration times of 30–100 ms/spectrum.

Structural changes observed with AFM while imaging the polymer films can be linked with the chemical composition from Raman imaging, thus leading to the correlation between chemical composition data and the constructional morphology of the films. Furthermore, due to its confocal setup, the confocal Raman microscope can be used to determine the layered structure of polymer coatings without laborious sample preparation as shown in Sect. 20.4. Additionally, the detection of inorganic materials in a polymer matrix was demonstrated in Sect. 20.5.

Confocal Raman microscopy (especially in combination with AFM) allows the nondestructive characterization of heterogeneous materials. In combination with a suitable software package, chemical identification of sample volumes of only 0.004 μm^3 becomes available at integration times of less than 100 ms per spectrum.

References

1. W. Stocker, J. Beckmann, R. Stadler, J. Rabe, Macromolecules **29**, 7502 (1999)
2. N. Koneripalli, R. Levicky, F.S. Bates, J. Ankner, H. Kaiser, S.K. Satija, Langmuir **12**, 668 (1996)
3. T.J. Morkved, H.M. Jaeger, Europhys. Lett. **40**, 643 (1997)
4. T.S. McLean, B.B. Sauer, J. Polym. Sci. Part B **37**, 85 (1999)
5. T. Zhong, D. Inniss, K. Kjoller, V. Ellings, Surf. Sci. **290**, L688 (1993)
6. S.N. Magonov, V. Elings, M.H. Whangbo, Surf. Sci. **372**, L385 (1997)
7. J. Tamayo, R. Garcia, Appl. Phys. Lett. **71**, 2394 (1997)
8. J. Tamayo, R. Garcia, Appl. Phys. Lett. **73**, 2926 (1998)
9. R. Garcia, J. Tamayo, A. Paolo, Surf. Interface Anal. **27**, 312 (1999)
10. J.P. Cleveland, B. Anczykowski, A.E. Schmid, V.B. Elings, Appl. Phys. Lett. **72**, 2613 (1998)
11. W.W. Scott, B. Bhushan, Ultramicroscopy **97**, 151 (2003)
12. G. Bar, Y. Thomann, R. Brandsch, H.J. Cantow, M.H. Whangbo, Langmuir **13**, 3807 (1997)
13. S. Hild, O. Marti, F. Hollmann, B. Rieger, Europ. Polym. J. **40**, 905 (2004)
14. H.W. Siesler, K. Holland-Moritz, *Infrared and Raman Spectroscopy of Polymers* (Marcel Dekker, New York, 1990)
15. H. Owen, D.E. Battery, M.J. Pelletier, J.B. Slater, SPIEE Proc. **260**, 2406 (1995)
16. E.D. Lipp, R.L. Grosse, Appl. Spectrosc. **52**, 42 (1998)
17. J.F. Aust, K.S. Booksh, M.L. Myrick, Appl. Spectrosc. **50**, 382 (1996)
18. T. Wilson, *Confocal Microscopy* (Academic Press, London, 1990)
19. J.M. Chalmers, H.G.M. Edwards, J.S. Lees, D.A. Long, M.W. Mackenzie, H.A. Willis, J. Raman Spectrosc. **22**, 613 (1991)
20. X. Wang, S. Michielsen, J. Appl. Polym. Sci. **82**, 1330 (2001)
21. A.S. Nielsen, D.N. Batchelder, R. Pyrz, Polymer **43**, 2671 (2002)
22. G.R. Strobl, W. Hagedorn, J. Polym. Sci. Polym. Phys. **16**, 1181 (1978)
23. R. Mutter, W. Stille, G. Strobl, J. Polym. Sci. Pol. Phys. **31**, 99 (1993)

24. P. Hendra, J. Vile, H.A. Willis, V. Zichy, Polymer **25**, 785 (1984)
25. G. Keresztury, E. Foldes, Polym. Test **9**, 329 (1990)
26. E. Lamparska, V. Liegeois, O. Quinet, B. Champagne, ChemPhysChem **7**, 2366 (2006)
27. V.K. Kuppa, J. in't Veld, G.C. Rutledge, Macromolecules **40**, 5187 (2007)
28. K. Tashiro, S. Minami, G. Wu, M. Kobayashi, J. Polym. Sci. Polym. Phys. **30**, 1143 (1992)
29. J.C. Rodriguez-Cabello, J.C. Merino, T. Jawhari, J.M. Pastor, J.M. Pastor, J. Raman Spectrosc **27**, 463 (1996)
30. L. Holliday, *Structure and Properties of Oriented Polymers* (Applied Science Publishers, London UK, 1975), chap. 7
31. S. Hild, A. Rosa, O. Marti, *Scanning Probe Microscopy of Polymers* (Oxford University Press, 1998), p. 110
32. P. Schmidt, J. Dybal, J. Scudla, M. Raab, J. Kratochvil, K. Eichhorn, S.L. Quintana, J.M. Pastor, Macromol. Symp. **184**, 107 (2002)
33. H. Tadokoro, H. Kobayashi, M. Ukita, K. Yasufuku, S. Murahashi, J. Chem. Phys. **42**, 1432 (1965)
34. R.G. Snyder, J.H. Schachtschneider, Spectrochim. Acta **20**, 853 (1964)
35. U. Schmidt, S. Hild, W. Ibach, O. Hollricher, Macromol. Symp. **230**(1), 133 (2005)
36. L. Utracki, *Encyclopaedic Dictionary of Commercial Polymer Blends* (ChemTec Publishing, Toronto, 1994)
37. L. Utracki, *Polymer Blends Handbook* (Kluwer Academic Publishers, Dordrecht, 2002)
38. U. Schmidt, W. Ibach, J. Mueller, O. Hollricher, SPIEProc. **6616**(1), 66160E (2007)
39. H. Kupsov, G.N. Zhizhin, *Handbook of Fourier Transform Raman and Infrared Spectra of Polymers* (Elsevier, Amsterdam, 1998)
40. G. Socrates, *Infrared and Raman Characteristic Group Frequencies* (Wiley, Chichester, 2001)
41. Z.O. Oyman, W. Ming, F. Micciche, E. Oostveen, J. van Haveren, R. van der Linde, Polymer **45**, 7431 (2004)
42. M. Milnera, J. Kürti, M. Hulman, H. Kuzmany, Phys. Rev. Lett. **48**, 1324 (2000)
43. A. Jorio, R. Saito, J.H. Hafner, C.M. Lieber, M. Hunter, T. McCluve, G. Dresselhaus, M.S. Dresselhaus, Phys. Rev. Lett. **86**, 1118 (2001)